BIOORGANIC CHEMISTRY 15, 183–193 (1987)

^1H and ^{13}C NMR Spectra, Protonation, Deprotonation, and Host–Guest Complexation-Induced Shifts of Some Fluorescence Dyes[1]

HANS-JÖRG SCHNEIDER[2] AND JÜRGEN PÖHLMANN

FR Organische Chemie der Universität des Saarlandes, D-6600 Saarbrücken 11, Germany

Received August 28, 1986

^1H and ^{13}C NMR signal assignments for 8-anilinonaphthalenesulfonic acid (ANS) and dansyl amide (DNSA) are achieved using high-field spectra, decoupling, and two-dimensional NMR techniques as well as shift differences between conjugate acid and bases. Complexation of ANS and DNSA with a macrocyclic azoniacyclophane is measured by fluorescence and by NMR shift titration, furnishing an independent check for the equilibrium constant determination. The complexation-induced shifts (CIS) for ANS and DNSA are analyzed on the basis of aromatic ring current and linear electric field effect models. Comparison of equilibrium constants of the cyclophane and different substrates shows that, e.g., for ANS, lipophilic/hydrophobic binding dominates over electrostatic effects despite the presence of charges and the absence of a lipophilic cap or bottom on the receptor molecule.

Fluorescence dyes such as 8-anilinonaphthalene-1-sulfonic acid (ANS, Scheme 1) or 5-dimethylaminonaphthalene-1-sulfonamide (dansylamide, DNSA) are often used as biochemical probes to detect the presence of a lipophilic or hydrophobic environment in protein pockets, which leads to distinct fluorescence or quantum yield enhancement (*2*). The high sensitivity of this spectroscopic technique allows the determination of large binding constants with suitable receptors. It is also for this reason that the use of, e.g., ANS has become popular in the investigation of macrocyclic host compounds as receptor or enzyme analogs (*3*). Little, however, is known about the geometry of complexes with such dyes and about the different binding contributions. Molecules such as ANS may well bind primarily because of electrostatic attractions with their negatively charged sulfonic acid groups, even in an acidic environment, although the observed fluorescence effect indicates an unpolar environment.

NMR spectroscopy is expected to shed light on the questions raised above. The manifold NMR signals and their shielding differences upon complexation which are accessible by modern NMR techniques (*4*) relate to conformational properties of host–guest complexes in a more direct way than other spectroscopic techniques; electrostatic effects due, e.g., to protonation/deprotonation are also easily

[1] This paper is Part 10 of the series Host–Guest Chemistry. For Part 9, see Ref. (*1*).

[2] To whom correspondence should be addressed.

0045-2068/87 $3.00

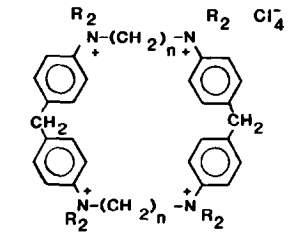

CP66: R=Me, n=6

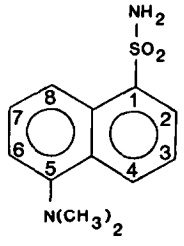

DNSA

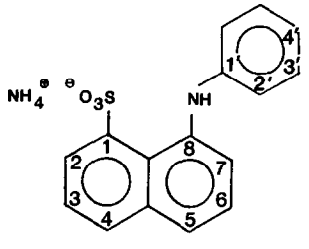

ANS

Equilibrium contant, K

	In 100% D_2O	In 50% CD_3OD	In 80% CD_3OD
DNSA	0.05 (Fluor.)	0.016 (NMR)	—
ANS	4.0 (Fluor.)	0.33 (Fluor.)	0.13 (Fluor.) 0.096 (NMR)

SCHEME 1. Structures and complexation equilibrium constants K (in 10^5 liters/mol; average error, ±15%), in CD_3OD/D_2O at 25 ± 3°C. Methods: Fluorescence (Fluor.) and/or ^1H NMR titration. Average K values from all ^1H NMR signals with $(\vartheta_{cplx} - \vartheta_o) > 0.3$ ppm; see Table 1.

recognized by NMR. ^1H NMR shifts for ANS were reported earlier (*2e*), on the basis of older methods; there are new assignments in the present paper.

As a first step in this direction we analyze the ^1H and ^{13}C NMR spectra of ANS and DNSA, measure their complexation shifts in a well-defined host[3] environment, and finally provide—to our knowledge for the first time—a check of equilibrium constants obtained from fluorescence spectroscopy by an independent NMR-shift titration.

RESULTS

DNSA: Protonation- and Deprotonation-Induced Shifts

The 400-MHz ^1H NMR spectrum of DNSA shows four well-separated doublets and two heavily overlapping multiplets (Fig. 1, see Table 1); the observed cou-

[3] Preliminary report: Ref. (*5*). Also see Ref. (*3b*) and references cited therein for earlier related examples.

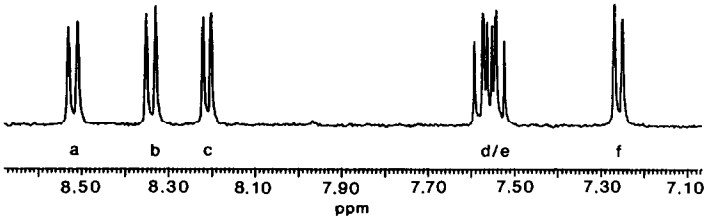

FIG. 1. ^{1}H NMR (400 MHz) spectrum of DNSA (~5% in $CDCl_3/d_6$-DMSO = 4/1).

pling constants (Table 2) and decoupling experiments established vicinal connectivity between signals a and d, b and e, f and e. Known substituent effects of SO_2NH_2 and NMe_2 groups in benzene (*6*) show that signals a and c belong to the sulfonamide substituted ring. Differentiation, however, between a and c, and particularly between b and f required additional arguments.

Shielding differences between conjugate acid and bases provide a convenient tool for signal assignments (*7*), particularly in aromatic systems where simple

TABLE 1

^{1}H AND ^{13}C NMR: PROTONATION-INDUCED SHIFTS (PIS), DEPROTONATION-INDUCED SHIFTS (DIS), AND CP66–COMPLEX SHIFTS (Cplx)[a]

	1	2	3	4	5	6	7	8	9	10
DNSA										
^{1}H/50%[b]	—	8.51	7.67	8.26	—	7.40	7.69	8.30	—	—
^{1}H/PIS	—	[c]	0.09[d]	0.125	—	0.33	0.09[d]	0.24	—	—
^{1}H/DIS	—	−0.24	−0.15	−0.71	—	−0.11	[c]	0.27	—	—
^{1}H/Cplx[e]	—	7.89	6.85	7.62	—	6.75	6.75	7.94	—	—
^{13}C/DMSO[f]	139.7	123.5	127.6[d]	129.0[d]	151.3	115.3	126.4[d]	119.6	129.0	126.4
ANS[g]										
^{1}H/80%[h]	—	8.34	7.42	7.94	7.49	7.40	7.56	—	—	—
^{1}H/Cplx 80%[h]	—	7.49	6.57	7.56	7.18	6.40	6.33	—	—	—
^{1}H/20%[i]	—	8.33	7.55	8.10	7.69	7.53	7.67	—	—	—
^{1}H/Cplx 20%[i]	—	7.03	6.17	7.26	6.80	5.61	5.45	—	—	—
^{13}C/80%[h]	[c]	118.3	124.9	123.0	134.2	127.2	128.8	146.1	123.8	138.5

[a] In ppm ± 0.003 (for ^{1}H) or ± 0.05 (for ^{13}C), vs tetramethylsilane (TMS) (calculated with ϑ = 3.40 from internal CHD_2OD, which was used as internal reference), unless noted otherwise. Ambient temperature; PIS, DIS: shifts relative to the neutral compound.

[b] In 50% CD_3OD/D_2O (vol + vol); Me signal, 2.87.

[c] Not measured (due to signal overlap, etc.).

[d] Indistinguishable or/and overlapping signals.

[e] Calculated for fully complexed substrate. Average error, ± 0.05 ppm. In 50% CD_3OD/D_2O (vol + vol). Me signal, 2.79.

[f] ~10% in d_6-dimethyl sulfoxide. Internal reference, TMS. Me signal, 45.0.

[g] Phenyl signals in ANS (in 80% CD_3OD/D_2O) in the order H/C 2′, 3′, 4′: 7.15, 7.23, 6.84 (Cplx: 6.73, 7.12, 6.87) all ^{1}H; ^{13}C: 118.3, 130.0, 120.8.

[h] In 80% CD_3OD/D_2O (vol + vol). For Cplx, cf. footnote *e*.

[i] In 20% CD_3OD/D_2O (vol + vol). For Cplx, cf. footnote *e*.

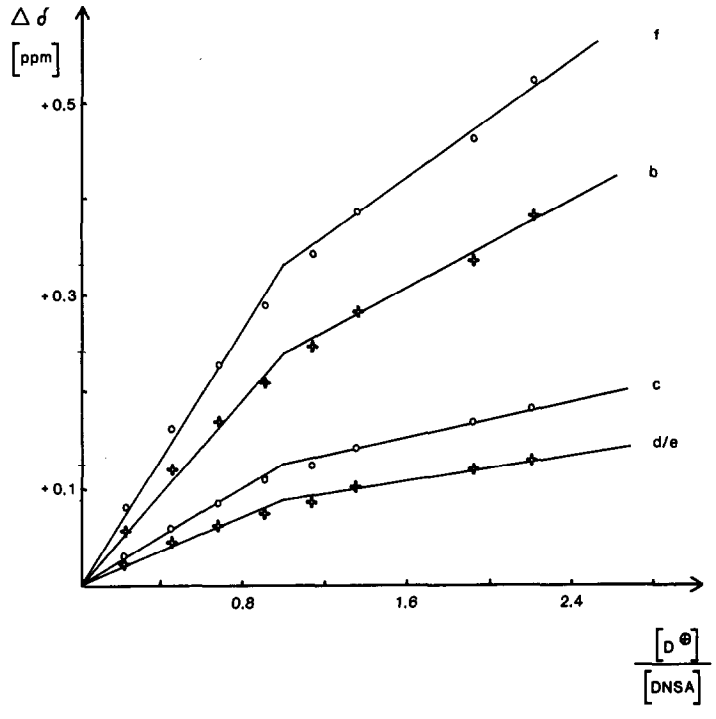

FIG. 2. ^{1}H NMR shift titration of DNSA with CF_3COOD (a 7.3×10^{-2} M CF_3COOD solution was added to 4.25×10^{-3} M DNSA, solvent d_6-DMSO/D_2O = 2/1).

reasoning allows differentiation among *o*, *m*, and *p* positions. Titration of DNSA with trifluoroacetic acid (Fig. 2, Table 1) clearly shows deshielding effects decreasing in the order of signals f (*o* position to NMe_2), b (*p*), c (benzylic), and d/e (*m* and other positions). The deshielding effects beyond the equivalence point of 1.0 (Fig. 2) result from further protonation at the amide or aromatic part of the molecule.

*De*protonation of DNSA (Fig. 3) supports the assignment of signal a to the *o*

TABLE 2

^{1}H–^{1}H COUPLING CONSTANTS (Hz)[a]

	H									
	2–3	2–4	3–4	5–6	5–7	6–7	7–8	2′–3′	3′–4′	2′–4′
ANS[b]	7.3	1.4	8.1	7.8	1.4	8.0	—	8.7	6.8	1.2
DNSA[c]	8.3	1.2	7.1	—	—	7.5	8.9	—	—	—

[a] ± 0.15 Hz, ambient temperature.
[b] In 80% CD_3OD/D_2O (vol + vol).
[c] In 50% CD_3OD/D_2O (vol + vol).

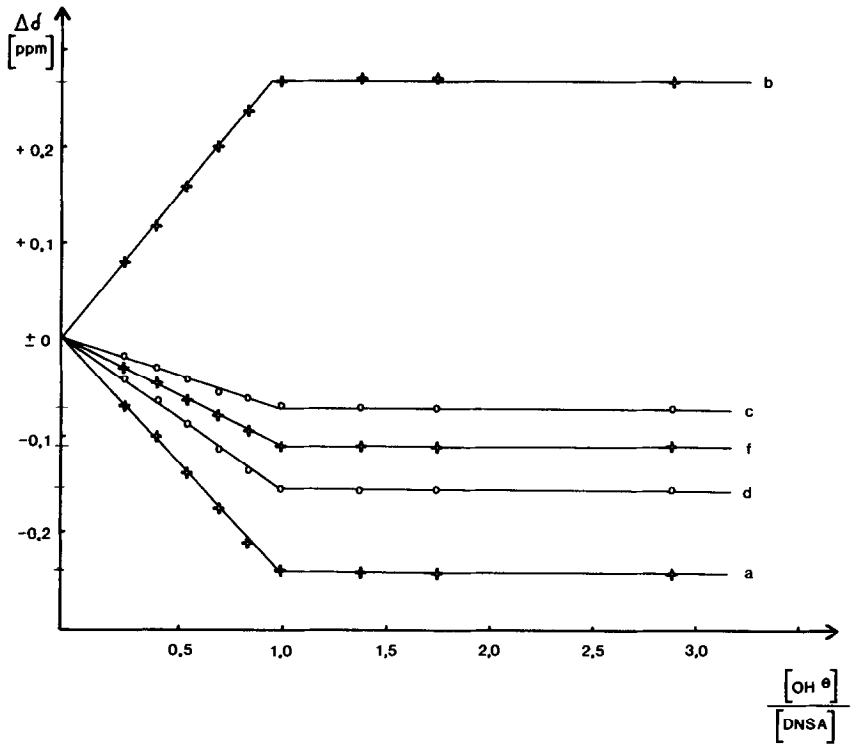

FIG. 3. ^{1}H NMR shift titration of DNSA with NaOD (4×10^{-2} M NaOD added to 10^{-2} M DNSA in d_6-DMSO/D_2O = 2/1.

position 2; the absence of through conjugation from the SO_2NH^- group manifests itself in the smallest shielding effect on the *p* position 4 (Table 1). Noteworthy, the largest, and *de*shielding effect is found for H-8, clearly pointing to a through-space electric field effect between the approximately parallel C1–SO_2NH^- dipole and the C8–H8 bond. The relatively high acidity of the sulfonamide group [p$K_s \sim 9.8$ (*8*)] renders deprotonation of a fluorescence probe such as DNSA in proteins possible; the shielding differences discussed can shed light on corresponding binding contributions. ^{13}C signal assignments were accomplished by DEPT (*4*) experiments and by substituent induced shift (*6*) calculations.

ANS: Assignment by Two-Dimensional NMR Spectroscopy

The nine proton signals of ANS show so much overlapping, even at 400 MHz, that two-dimensional NMR techniques for signal assignment are safer and more economical than are conventional techniques. As the most useful method[4] we used ^{13}C–^{1}H shift correlated spectroscopy (*4*), which of course required the as-

[4] For a recent discussion of suitable two-dimensional methods for complicated spin systems, see Ref. (*9*).

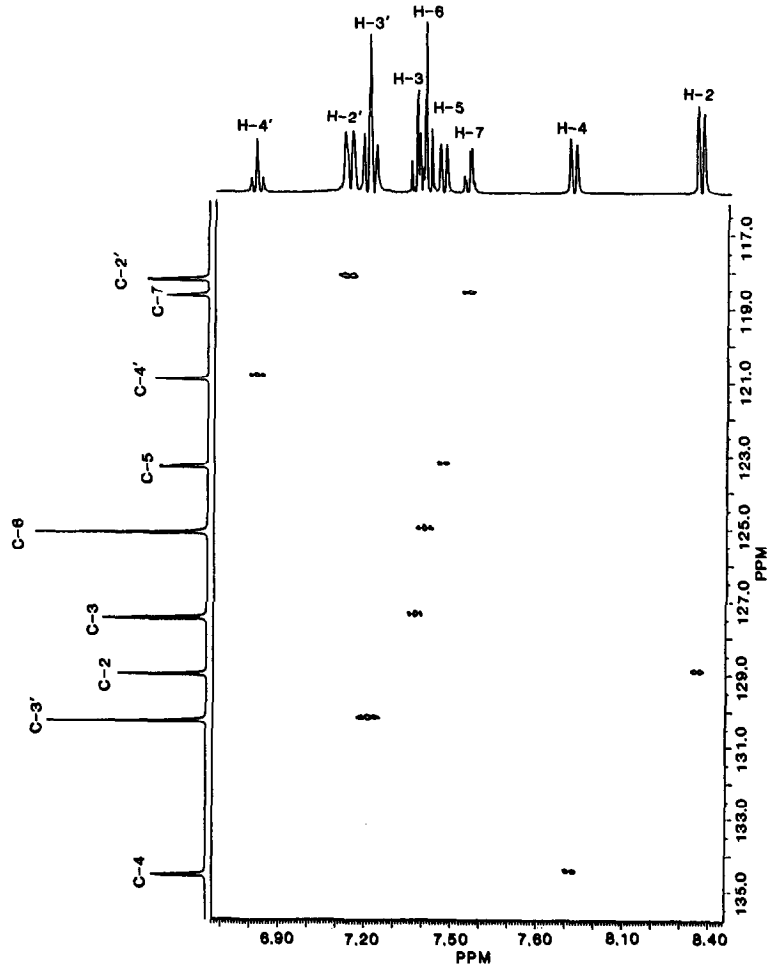

FIG. 4. ^{13}C–^{1}H Shift correlation of ANS, ^{1}H and ^{13}C NMR spectra, and cross section [50 mg ANS in 1 ml CD_3OD/D_2O = 4/1; small shift deviations from data in Table 1 are due to the high concentration used for the two-dimensional experiment; one bond coupling emphasized; other measuring conditions as in Ref. (*9*)].

signment of 14 nonequivalent ^{13}C signals. This was achieved on the basis of multiplicities obtained from DEPT (*4*) spectra (not shown) and known substituent effects (*6*) in benzenes bearing amino and sulfonic acid groups. However, for safe assignments the carbon signals attributed to C-3/C-4, C-6/C-7, and C-2′–C-3′ were either too close (C-3/C-4) or too far away from shift calculations with single substituent parameters (due to deviations from additivity). In this case the multiplicity seen in ^{13}C–^{1}H cross section (Fig. 4) allowed unambiguous assignment, since the peaks corresponding to H-3, H-6, and H-3′ are recognized as doublets of doublets, whereas H-4, H-7, and H-2′ are clearly doublets, as to be expected from the structural connectivity.

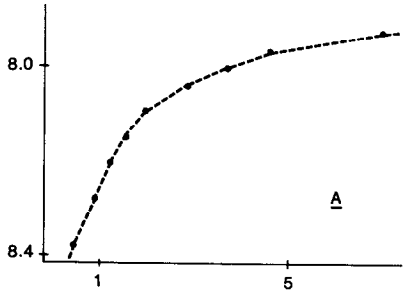

FIG. 5. An example for ^{1}H NMR complex titration: DNSA with CP66. (A) Observed H-2 shifts (ppm) vs CP66 concentration (in 10^3 M). (B) Scatchard control plot. Measured in 50% (vol + vol) CD_3OD/D_2O. Parameters obtained from fitting to curve A: $K = (1.56 \pm 0.15) \times 10^3\ M^{-1}$; ϑ for 100% complexation, 7.89 ± 0.002 ppm from TMS.

Complexation of DNSA and ANS with CP66

Constants for complexation with CP66 (Scheme 1) were obtained by fluorescence titration for ANS and DNSA in different aqueous mixtures (*5*), and for ANS also by ^{1}H NMR titration in 80% CD_3OD/D_2O. Figures 5 shows a representative example; a Scatchard plot (*10*) was used only for linearity control after obtaining the parameters for the unknowns (equilibrium constant K_a and intrinsic shift or fluorescence intensity value of the fully complexed substrates) by a nonlinear least-squares fitting. Details of the methods, errors, and comparisons with other substrates will be published elsewhere (*11*), but the K values given in Scheme 1 are believed to be accurate to approximately ±10%; the NMR complexation shifts (Table 1) to ±0.05 ppm on the average. It is gratifying that the equilibrium constants for ANS obtained from fluorescence and ^{1}H NMR titration agree within the error included in both determinations (Scheme 1).

The complexation-induced ^{1}H NMR shifts (CIS) amount to as much as 2 ppm shielding for H-6 and H-7 in ANS, whereas, for the anilino proton, the CIS are below 0.5 ppm, down to 0.1 ppm at the *p* position 4′. These observations indicate that the naphthalene part must be immersed in the *CP66* cavity, which is also supported by similar results with DNSA (Table 1) (*5, 11*). The strong increase in CIS with increasing water content of the solvent (Table 1) is indicative of a stronger substrate fixation with increasing complexation free energy and will be discussed in the context of numerous other examples (*11*).

The most important conclusion made from the observed binding constants (*5*) (Scheme 1) is that even for the negatively charged ANS, lipophilic/hydrophobic binding dominates over of course sizable electrostatic contributions, although the substrate is surrounded by four positive host charges and the receptor CP66 has no lipophilic bottom or cap for the inclusion. The predominance of lipophilic over electrostatic contributions emerges both from the comparison of binding free enthalpies (ΔG^0 kJ/mol) in D_2O for ANS, e.g., 29, for DNSA, 20, and for naphthalene 17 (*5*) and from the observed solvent dependence (*5*), which for ANS also shows increased binding with decreasing methanol content.

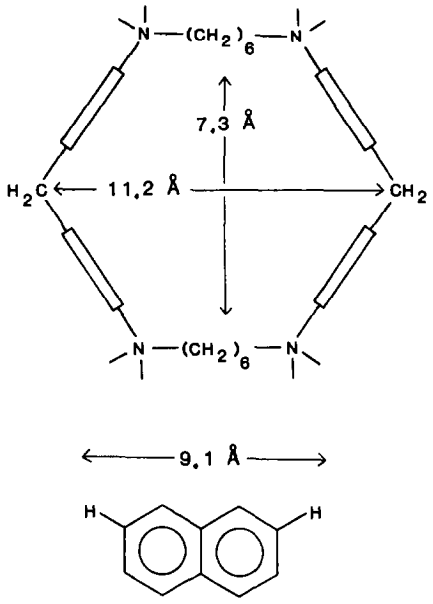

SCHEME 2. Basic geometry for the CP66–naphthalene complex.

NMR Shielding Calculations

The calculation of complexation-induced NMR shifts on naphthalene as model substrate within the CP66 cavity was based on a simplified conformation, in which all methylene carbon atoms and all nitrogen atoms were placed in one plane (Scheme 2) with the phenyl ring perpendicular to this plane. An orthogonal Cartesian coordinate system was introduced with the axis x cutting through the benzylic methylene atoms; the origin in one benzylic carbon atom, the y axis in and the z axis perpendicular to the macroring plane. The atom positions were obtained using intraannular distances taken from Dreiding models (shown in Scheme 2) and standard bond length and angles together with suitable coordinate and trigonometric transformations.

As major contributions, ring current anisotropy effects ($\Delta\chi$) from the CP66–benzene parts and linear electric field effects (E_z) from the charged ammonium groups were calculated using tabulated values (*12*) for $\Delta\chi$ and a parametrization for E_z as described earlier (*9*). The $\Delta\chi$ and E_z contributions were calculated for each atom in inserted naphthalene and averaged afterward. Table 3 gives the obtained complexation-induced shifts calculated for a symmetric equatorial and axial inclusion of naphthalene, where the orientation refers to the major axis of the substrate. In line with CPK-model inspections the naphthalene plane was oriented perpendicular to the macroring. CIS for pseudoaxial inclusion of the substrate (Table 3) were obtained as averages from equatorial and axial orientations.

Calculations of CIS at this level can provide only first approximations. Besides neglect of other contributions, such as from gegenions E_z, from medium effects,

TABLE 3

CALCULATED AND OBSERVED ^{1}H NMR COMPLEXATION-INDUCED SHIFTS[a] IN CP66

	α-H			β-H					
Orientation	Δχ	E_Z	Sum	Δχ	E_Z	Sum			
Equatorial	−1.00	0.58	−0.42	−1.32	−0.58	−1.90			
Axial	−2.58	−0.36	−2.94	−0.50	−0.70	−1.20			
Pseudoaxial[b]	—	—	−1.68	—	—	−1.55			
Observed[c]	—	—	−0.85	—	—	−1.7			
	C-1			C-2			C-9		
	Δχ	E_Z	Sum	Δχ	E_Z	Sum	Δχ	E_Z	Sum
Equatorial	−1.92	0.28	−1.64	−3.78	0.50	−3.28	−2.04	0.68	−1.36
Axial	−2.20	0.48	−1.72	−1.06	0.20	−0.86	−2.34	0.68	−1.66
Pseudoaxial[b]	—	—	−1.68	—	—	−2.07	—	—	−1.51

[a] Model calculations for naphthalene. Δχ = anisotropy contribution from aromatic ring currents, E_Z = linear electric field effect contribution (from N^+). All values in ppm. See text.

[b] Average of equatorial and axial orientations.

[c] Average values for ANS (see Table 1) in 20% (vol + vol) CD_3OD/D_2O.

etc., the calculation is based on simplified values for benzene instead of anilinium systems, and the complex geometry is highly idealized. Nevertheless, the calculated values agree with total immersion of the naphthalene in the cavity; they allow exclusion of an axial or pseudoaxial orientation of the substrate, although the differences in CIS at H-2/H-3 (−1.35 ppm, average values) and H-6/H-7 (−2.1 ppm), as well as the small CIS at H-4/H-5 (−0.85 ppm) indicate a deviation from an equatorial inclusion. This would be the result of a deeper insertion of carbon atoms 5-6-7-8 in the cavity. Koga and co-workers (*13*) have reported NMR anisotropy effect calculations in a related cyclophane with naphthalene-1,8-diol. However, the numbers presented by the Japanese authors do *not* allow to exclude axial inclusion; moreover, our calculations (Table 3) indicate that the linear electric field effects exerted by the positive nitrogen atoms can be even larger than the aromatic anisotropy contributions; their neglect will therefore lead to large and systematical errors. In view of the many problems involved with the rigorous calculation of ^{1}H NMR shielding contributions, even with conformationally fixed substrates (*9*), it is gratifying that the first results presented at least allow differentiation of the parts of the substrate encapsulated within the host cavity and elimination of a predominantly axial inclusion.

EXPERIMENTAL AND COMPUTATIONAL DETAILS

ANS, DNSA, and solvents were the purest grades commercially obtainable. CP66-octamethyltetrachloride was prepared according to Ref. (*14*).

Fluorescence titrations were performed using a Perkin–Elmer MPF-44A instrument at 25°C; the excitation wavelengths for DNSA were 325 nm (H_2O), 330 nm (20% CH_3OH), and 340 nm (other solvents); that for ANS was 375 nm. Intensities were measured at 530 nm with DNSA and at 500 nm with ANS. The complexation-induced increase in fluorescence intensity (ΔI) as a function of [CP66]/[ANS] or [CP66]/[DNSA] allowed us to obtain equilibrium constants as usual (*2a, b, 10*), although a numerical curve fitting procedure (*5*) was used for the 1 : 1 complex with the substrate (*11*).

NMR measurements were carried out as described earlier (*9*), using a 400-MHz (^1H) Bruker AM400 system. NMR shift titrations were carried out similarly to the fluorescence titrations and evaluated by numerical curve fitting (*5, 11*).

ANS was measured in ~6 to 8 × 10^{-4} M solutions, DNSA in ~1.3 × 10^{-3} M solutions. No concentrations dependent shifts were observed, in contrast to an earlier investigation in which higher concentrations had to be used.

NMR shielding calculations were performed using tabulated ring-current anisotropy contributions (*12*) for $\Delta\chi$ and the modified Buckingham equation [Eq. (3) in Ref. (*9*)], using as polarizability 0.79 A^3 for C–H and 1.22 A^3 for C_{ar}–C_{ar} (*15*), and a point charge of 1 at N^+. The geometric calculations were based on the following standard parameters (*16*): bond angle, C–C–C (benzylic sp^3) 110°; distances (Å), C_{ar}–H 1.08, C_{ar}–C_{ar} 1.395, C–N^+ 1.43, C_{ar}–CH_2 1.52.

ACKNOWLEDGMENTS

This work was financially supported by the Deutsche Forschungsgemeinschaft, Bonn, and the Fonds der Chemischen Industrie, Frankfurt.

REFERENCES

1. SCHNEIDER, H.-J., AND SCHNEIDER, U., *J. Org. Chem.*, in press.
2. (*a*) UDENFRIEND, S. (1969) Fluorescence Assay in Biology and Medicine, Academic Press, New York/London; (*b*) Biochemical Fluorescence: Concepts (R. F. Chen and H. Edelhoch, Eds.), Dekker, New York/Basel, Vol. 1 (1975), Vol. 2 (1976); (*c*) STRYER L. (1968) *Science* **162,** 526; (*d*) DODIUK, KANETY, H., AND KOSOWER, E. M. (1979) *J. Phys. Chem.* **3,** 515, and references cited therein; (*e*) PENZER, G. R. (1972) *Eur. J. Biochem.* **25,** 218.
3. (*a*) BENDER, M. L., AND KOMIYAMA, M. (1978) Cyclodextrin Chemistry, Springer, Berlin; (*b*) ODASHIMA, K., AND KOGA, K. (1983) *in* Cyclophanes II (*Org. Chem. New York* **45**), p. 629; (*c*) TABUSHI, I. (1982) *in* Frontiers of Chemistry (IUPAC) (K. J. Laidler, Ed.), p. 275, Pergamon, Oxford; (*d*) SCHNEIDER, H.-J., BUSCH, R., KRAMER, R., AND SCHNEIDER, U. (1987) Advances in Chemistry, Amer. Chem. Soc., Washington, DC, in press.
4. (*a*) BENN, R., AND GÜNTHER, H. (1983) *Angew. Chem.* **95,** 381; (1983) *Angew. Chem. Int. Ed. Engl.* **22,** 390; (*b*) BAX, A. (1984) Two-Dimensional Nuclear Magnetic Resonance in Liquids, Delft Univ. Press, Dordrecht; (*c*) HULL, W. E., AND WEHRLI, F. W. (1984) *Top. Carbon-13 NMR Spectrosc.* **4,** 33; (*d*) MORRIS, G. A. (1984) *Top. Carbon-13 NMR Spectrosc.* **4,** 180; (*e*) BAX, A. (1984) *Top. Carbon-13 NMR Spectrosc.* **4,** 199.
5. SCHNEIDER, H.-J., PHILIPPI, K., AND PÖHLMANN, J. (1984) *Angew. Chem.* **96,** 907; (1984) *Angew. Chem. Int. Ed. Engl.* **23,** 908.
6. PRETSCH, E., CLERC, TH., SEIBL, J., AND SIMON, W. (1976) Tabellen zur Strukturaufklärung organischer Verbindungen, Springer, Berlin.

7. AGRAWAL, P. K., AND SCHNEIDER, H.-J. (1983) *Tetrahedron Lett.* **24,** 177.
8. CHEN, R. F., AND KERNOHAN, J. C. (1967) *J. Biol. Chem.* **242,** 5813.
9. SCHNEIDER, H.-J., BUCHHEIT, U., BECKER, N., SCHMIDT, G., AND SIEHL, U. (1985) *J. Amer. Chem. Soc.* **107,** 7027.
10. DAHLQUIST, F. W. (1978) *in* Methods of Enzymology (C. H. W. Hirs and S. N. Timasheff, Eds.), Vol. 48, Part F, p. 270, Academic Press, New York.
11. SCHNEIDER, H.-J., KRAMER, R., PHILIPPI, K., PÖHLMANN, J., AND THEIS, I., manuscript in preparation.
12. BOVEY, F. B. (1969) Nuclear Magnetic Resonance Spectroscopy, pp. 64, 264, Academic Press, New York/London.
13. ODASHIMA, K., ITAI, A., IITAKA, Y., ARATA, Y., AND KOGA, K. (1980) *Tetrahedron Lett.* **21,** 4347.
14. SCHNEIDER, H.-J., AND PHILIPPI, K., (1984) *Chem. Ber.* **117,** 3056.
15. LEFÈVRE, J. W., AND STEEL, K. D. (1961) *Chem. Ind.,* 670.
16. WEAST, R. C. (Ed.) (1972) Handbook of Chemistry and Physics, Chemical Rubber Co., Cleveland, Ohio p. F-179 ff.